Available online at www.sciencedirect.com

ScienceDirect

Procedia IUTAM 19 (2016) 65 – 74

Procedia IUTAM

www.elsevier.com/locate/procedia

IUTAM Symposium Analytical Methods in Nonlinear Dynamics

Nonlinear Vibration Absorber Optimal Design via Asymptotic Approach

Arnaldo Casalotti[a], Walter Lacarbonara[a]

[a]*Sapienza University of Rome, Department of Structural and Geotechnical Engineering, Via Eudossiana 18, 00184 Rome, Italy*

Abstract

This paper tackles the classical problem of Vibration Absorbers (VAs) operating in the nonlinear dynamic regime. Since traditional linear VAs suffer from the drawback of a narrow bandwith and numerous structures exhibit nonlinear behavior, nonlinear absorbers are of practical interest. The resonant dynamic behavior of a nonlinear hysteretic VA attached to a damped nonlinear structure is investigated analytically via asymptotics and numerically via path following. The response of the reduced-order model, obtained by projecting the dynamics of the primary structure onto the mode to control, is evaluated using the method of multiple scales up to the first nonlinear order beyond the resonance. Here, the asymptotic response of the two-degree-of-freedom system with a 1:1 internal resonance is shown to be in very close agreement with the results of path following analyses. The asymptotic solution lends itself to a versatile optimization based on differential evolutionary.

Peer-review under responsibility of organizing committee of IUTAM Symposium Analytical Methods in Nonlinear Dynamics

Keywords: Asymptotics, Multiple time scales, Hysteresis, Bouc-Wen, Tuned Mass Damper, Vibration Control

1. Introduction

The suppression of unwanted vibrations and the mitigation of large-amplitude oscillations experienced by engineering structures via passive control strategies are widely investigated in the literature. First introduced by Frahm[1], the linear vibration absorber (VA) is the most common device to suppress the oscillations suffered by a structure. Approximate formulas were derived in[2,3] for the VA optimal stiffness and damping by the use of the equal peak method. More recently, a closed-form exact solution for the linear absorber was obtained in[4].

Nonlinear absorbers are also widely studied, including auto-parametric oscillators[5,6,7] and nonlinear energy sinks[8,9]. The autoparametric VA was first proposed in[5] where the behavior of a two-degree-of-freedom (two-dof) system subject to harmonic excitation was studied according to a first order asymptotic approximation which allowed to investigate the absorber performance. In[6] the method of multiple scales was adopted to study the behavior of a pendulum-like absorber attached to a linear spring-dashpot oscillator under a 2:1 internal resonance. A study of a nonlinear energy

* Walter Lacarbonara.
E-mail address: walter.lacarbonara@uniroma1.it

Peer-review under responsibility of organizing committee of IUTAM Symposium Analytical Methods in Nonlinear Dynamics
doi:10.1016/j.piutam.2016.03.010

sink was proposed in [9] where the method of multiple scales together with the harmonic balance method were employed to investigate the capability of this device to control chatter-induced vibrations. Such devices have the potential to damp oscillations over an extended frequency bandwidth, yet they exhibit a number of drawbacks. In particular, the auto-parametric absorber is capable of extracting energy from the primary system only if the forcing amplitude exceeds a certain threshold. Likewise, nonlinear energy sinks may be effective only if the input energy is above a characteristic threshold level.

A tuning methodology for nonlinear absorbers was proposed in [10] based on the imposition of the equality of the energy possessed by the vibrating element and by the absorber, considering also the case of essentially nonlinear systems. The equal peak method was adopted in [11,12] together with the harmonic balance method truncated to the first harmonic component to derive an optimal approximate tuning formula for a nonlinear absorber attached to a Duffing oscillator. In [12] it was pointed out that the constitutive law of the absorber must exhibit the same nonlinearity of the primary system.

Unlike linear absorbers, nonlinear devices are strongly influenced by the external excitation and their performance can suffer the drawback of strong detuning as the forcing amplitude varies. In [13] extensive numerical and experimental investigations were conducted on nonlinear absorbers where a hysteretic restoring force was introduced by means of steel wire ropes, whereas in [14,15] the introduction of hybrid NiTiNOL-steel wire ropes allowed to study also the pinching phenomenon and a larger optimization problem. It is of great interest to study the nonlinear regime by analytical techniques such as the method of multiple scales so as to investigate the behavior of the system for increasing levels of approximation. In [16,17] the method of multiple scales [18] was employed to derive the slow modulation of the amplitudes and phases of one-dimensional distributed-parameter nonlinear systems with quadratic and cubic nonlinearities, whereas a general procedure was developed in [19] to construct the nonlinear normal modes of self-adjoint structural systems.

In this study, the method of multiple scales is adopted to investigate the 1:1 internal resonance arising in a two-dof system composed of a nonlinear oscillator coupled with a nonlinear VA exhibiting hysteresis. The equations of motion derived via a Lagrangian approach are solved for different values of the characteristic parameters of the control device. Before discussing the performance of the control system, the behavior of the hysteretic absorber is investigated via the method of multiple scales. Such asymptotic method is then extended to the two-dof system to study the vibration control problem and to exploit the analytical solution within an optimization scheme.

2. Hysteretic Oscillator

In this section, the asymptotic analysis of a hysteretic oscillator subject to harmonic excitation is presented. The restoring force is the sum of linear and cubic elastic terms and a hysteretic part described by the Bouc-Wen model represented by a first-order nonsmooth evolution law. The equations of motion derived by a Lagrangian approach are here presented in nondimensional form as

$$\ddot{x} + \delta\, x + (1-\delta)\, z + \alpha\, x^3 = f \cos \Omega t, \tag{1}$$

$$\dot{z} = \left[1 - (\gamma + \beta\, \mathrm{sign}[z\,\dot{x}]|z|^n\right]\, \dot{x} \tag{2}$$

where the overdot $(\dot{})$ denotes differentiation with respect to the nondimensional time $t = \bar{\omega} t_{\mathrm{dim}}$. The characteristic frequency $\bar{\omega}$ is associated with the linear tangent stiffness of the oscillator. The parameter δ represents the ratio between the post-elastic stiffness and the linear tangent stiffness at the origin. The state-space formulation is adopted to express the equations of motion as first-order equations, by setting $q = x$ and $p = \dot{x}$. The state-space form of the nondimensional equations of motion is thus expressed as

$$\begin{aligned} &\dot{q} - p = 0, \\ &\dot{p} + q + \alpha\, q^3 + (1-\delta) z_{\mathrm{nl}} = f \cos \Omega t \end{aligned} \tag{3}$$

where z_{nl} represents only the nonlinear part of the hysteretic force, since its linear term is absorbed by the linear stiffness.

2.1. Piecewise representation

The steady-state response of the system to harmonic excitation allows to obtain the force-displacement hysteresis loop (see Fig. 1). Its shape is characterized by the constitutive parameters β and γ, while the smoothness of the transition between the elastic and post-elastic phases is governed by n. By setting $n = 1$, one can rewrite Eqn. (2) as

$$\frac{\partial z}{\partial x} = 1 - \{\gamma + \beta\,\mathrm{sign}\,[z\dot{x}]\}\,|z|. \tag{4}$$

The hysteretic cycle (see Fig. 1) can be divided into four different branches, each of them corresponding to a different

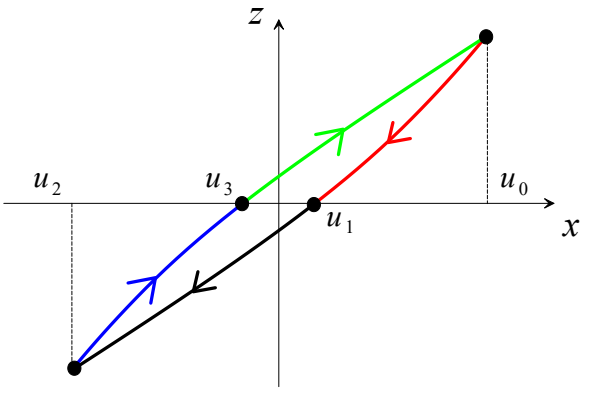

Fig. 1. Typical force-displacement hysteretic cycle. The four branches are highlighted by the red, black, blue and green solid lines and the transition points are described by the characteristic displacements u_i, $i = 0, 1, 2, 3$.

sign of the hysteresis function z multiplied by the velocity $\dot{x}$: branch 1 with $z \geq 0$, $\dot{x} \leq 0$ (red line in Fig. 1); branch 2 with $z < 0$, $\dot{x} < 0$ (black line in Fig. 1); branch 3 with $z < 0$, $\dot{x} > 0$ (blue line in Fig. 1); branch 4 with $z > 0$, $\dot{x} > 0$ (green line in Fig. 1).

The upper and lower bounds of the displacement during the steady-state periodic response are denoted by u_0 and u_2, respectively, while the displacements where the hysteretic force vanishes are denoted by u_1 and u_3. By considering the four branches with the corresponding signs, Eqn. (4) can be rewritten on each branch as

$$\begin{aligned} &\frac{\partial z_1}{\partial x} = -1 + (\gamma - \beta)\, z_1, \quad \text{with} \quad u_1 \leq x \leq u_0, \qquad -\frac{\partial z_2}{\partial x} = -1 + (\beta + \gamma)\, z_2, \quad \text{with} \quad u_2 \leq x < u_1 \\ &-\frac{\partial z_3}{\partial x} = 1 + (\beta - \gamma)\, z_3, \quad \text{with} \quad u_2 < x \leq u_3, \qquad \frac{\partial z_4}{\partial x} = 1 - (\beta + \gamma)\, z_4, \quad \text{with} \quad u_3 < x < u_0. \end{aligned} \tag{5}$$

These four equations are solved with respect to x to yield the expressions of z_i on the four branches as

$$z_1 = -\frac{1}{\beta - \gamma} + B_1 e^{x(\beta-\gamma)}, \quad z_2 = -\frac{1}{\beta + \gamma} - B_2 e^{x(\beta+\gamma)}, \quad z_3 = \frac{1}{\beta - \gamma} - B_3 e^{-x(\beta-\gamma)}, \quad z_4 = \frac{1}{\beta + \gamma} + B_4 e^{-x(\beta+\gamma)} \tag{6}$$

where B_i are constants. Next, the continuity of the hysteresis cycle at the transition points is enforced giving rise to the following six conditions:

$$z_1(u_0) - z_4(u_0) = 0, \qquad z_1(u_1) = z_2(u_1) = 0, \quad z_2(u_2) - z_3(u_2) = 0. \qquad z_3(u_3) = z_4(u_3) = 0. \tag{7}$$

Moreover, the symmetry of the cycle is prescribed according to $u_2 = -u_0$ so that u_0 represents here and henceforth the oscillation amplitude. Thus the four coefficients B_i and the displacements u_1 and u_3 can be expressed in terms of the oscillation amplitude u_0 and the z_i appearing in (6) are uniquely defined. Their expressions are then expanded in Taylor series of ϵ up to third order accounting only for the nonlinear part of the hysteretic force, since the linear part is absorbed in the linear stiffness. The power series expansion of $z^{(\mathrm{nl})}_{i,k} = z_{i,k} - x_k$ reads:

$$z^{(\mathrm{nl})}_i = \epsilon\, z^{(\mathrm{nl})}_{i,1} + \epsilon^2 z^{(\mathrm{nl})}_{i,2} + \epsilon^3 z^{(\mathrm{nl})}_{i,3}, \quad \text{with} \quad i = 1, \ldots, 4. \tag{8}$$

2.2. Multiple scales analysis

By introducing the small nondimensionsional parameter ϵ, the displacements and velocities are expressed in Taylor series of ϵ as

$$q = \epsilon\, q_1(t_0,t_1,t_2) + \epsilon^2\, q_2(t_0,t_1,t_2) + \epsilon^3\, q_3(t_0,t_1,t_2) \quad \text{and} \quad p = \epsilon\, p_1(t_0,t_1,t_2) + \epsilon^2\, p_2(t_0,t_1,t_2) + \epsilon^3\, p_3(t_0,t_1,t_2) \tag{9}$$

where $t_0 = t$ is the fast time scale and $t_1 = \epsilon\, t$ and $t_2 = \epsilon^2\, t$ are the slow time scales. According to these definitions, the time derivative becomes $d/dt = \partial_0 + \epsilon\partial_1 + \epsilon^2\partial_2$ with $\partial_j = \partial/\partial\, t_j$. Since it is of interest to study the nonlinear effects arising at higher orders, the external load is rescaled so as to appear at second order, $f = \epsilon^2 \bar{f}$. Therefore, the state-space form of the equations of motion gives rise to the following hierarchy of problems:

$$\begin{array}{lll} \text{Order } \epsilon: & \text{Order } \epsilon^2: & \text{Order } \epsilon^3: \\ \partial_0 q_1 - p_1 = 0 & \partial_0 q_2^{(i)} - p_2^{(i)} = -\partial_1 q_1 & \partial_0 q_3^{(i)} - p_3^{(i)} = -\partial_2 q_1 - \partial_1 q_2^{(i)} \\ \partial_0 p_1 + q_1 = 0 & \partial_0 p_2^{(i)} + q_2^{(i)} = f_2^{(i)} + f\cos\Omega t_0 & \partial_0 p_3^{(i)} + q_3^{(i)} = f_3^{(i)} \end{array} \tag{10}$$

The superscript i denotes the fact that at second and third orders, the hysteresis force assumes different expressions on the four branches during the oscillation period. This implies that also the solutions of the quadratic and cubic problems will assume different expressions along the hysteresis loop.

2.3. Linear Problem

The first order problem reduces to the linear undamped system whose solution is written in real form as

$$q_1 = a(t_1,t_2)\,\cos(t_0 + \theta(t_1,t_2)) \quad \text{and} \quad p_1 = -a(t_1,t_2)\,\sin(t_0 + \theta(t_1,t_2)) \tag{11}$$

where $a(t_1,t_2)$ denotes the oscillation amplitude coinciding with the linear approximation of u_0. Substituting Eqn. (11) into the second order problem yields the inhomogeneous terms from which the resonant terms must be eliminated in order to remove the singularity. To this end, further considerations on the periodicity of the problem are necessary.

The imposition of solvability requires the knowledge of the time instants at which the displacement of the first order problem attains the characteristic values u_i illustrated in Fig. 1. The first time instant to be determined is when the maximum value u_0 is attained, whereas the second time instant corresponds to the displacement u_1 which, in the linear approximation, coalesces to 0. These time instants can be obtained by imposing the following conditions:

$$\left.\frac{\partial q_1}{\partial t_0}\right|_{t_0=T_0} = 0 \;\Rightarrow\; T_0 = -\theta \quad \text{and} \quad q_1(t_0 = T_1) = 0 \;\Rightarrow\; T_1 = \frac{\pi}{2} - \theta. \tag{12}$$

The remaining time instants corresponding to the displacements u_2, u_3 and u_4, obtained by the periodicity of the linear solution as $T_2 = T_0 + \pi$, $T_3 = T_0 + 3\pi/2$, and $T_4 = T_0 + 2\,\pi$, are collected in the vector $\boldsymbol{\tau} = \{T_0,\, T_1,\, T_2,\, T_3,\, T_4\}$.

2.4. Higher Order Problems

To investigate the primary resonance, the closeness of the external excitation frequency and the natural frequency is expressed as $\Omega = 1 + \epsilon\sigma$. The inhomogeneous terms of the second order problem contain secular terms that must be eliminated. The solvability condition is obtained by imposing the orthogonality between the inhomogeneous terms $\mathbf{r}_2^{(i)}$ of the second order problem and the solution of the corresponding adjoint homogeneous problem that reads:

$$\begin{aligned} \partial_0 q^* - p^* &= 0, \\ \partial_0 p^* + q^* &= 0. \end{aligned} \tag{13}$$

The solvability conditions are thus expressed as

$$\sum_{i=1}^{4} \int_{\tau_i}^{\tau_{i+1}} \mathbf{w}_1^\top\, \mathbf{r}_2^{(i)}\, dt_0 = 0 \quad \text{and} \quad \sum_{i=1}^{4} \int_{\tau_i}^{\tau_{i+1}} \mathbf{w}_2^\top\, \mathbf{r}_2^{(i)}\, dt_0 = 0 \tag{14}$$

where $\mathbf{w}_1 = (\sin t_0, \cos t_0)$ and $\mathbf{w}_2 = (\cos t_0, -\sin t_0)$ represent the solutions of the adjoint problem. This way of enforcing the solvability stems from the piece-wise nature of the second order hysteretic restoring forces. The ensuing solvability conditions can be expressed as

$$\partial_1 a = -\frac{2\beta}{3\pi}(1-\delta)a^2 - \tfrac{1}{2} f \sin(\theta - \sigma t_1) \quad \text{and} \quad a\partial_1\theta = -\frac{2\gamma}{3\pi}(1-\delta)a^2 - \tfrac{1}{2} f \cos(\theta - \sigma t_1). \tag{15}$$

The second order problem incorporating the solvability conditions can be solved in a piece-wise fashion on each branch, thus leading to piece-wise expressions for $q_2^{(i)}$. A unique solution can be determined by imposing the continuity of the hysteresis cycle through the transition points and by enforcing its orthogonality to the solutions of the adjoint problem.

By substituting the second order solution into the third order problem, one obtains the corresponding inhomogeneous terms $\mathbf{r}_3^{(i)} = \{(-\partial_2 q_1 - \partial_1 q_2^{(i)}), f_3^{(i)}\}$. Again, the solvability is derived by enforcing the orthogonality between $\mathbf{w}_1, \mathbf{w}_2$ and $\mathbf{r}_3^{(i)}$, which leads to the expressions of $\partial_2 a$ and $\partial_2\theta$ that eliminate the resonant terms in the third order problem.

2.5. Modulation Equations

The system response can be studied by reconstituting the time derivatives of the amplitude and phase, thus arriving at the so-called modulation equations:

$$\dot{a} = \epsilon\partial_1 a + \epsilon^2\partial_2 a \quad \text{and} \quad \dot{\theta} = \epsilon\partial_1\theta + \epsilon^2\partial_2\theta. \tag{16}$$

Such equations are solved after transforming them into autonomous form. This can be done by introducing the relative phase (i.e., phase difference between the excitation and the response) $\psi = \sigma_1 t_1 - \theta$, thus obtaining

$$\begin{aligned} \dot{a} &= a^3 g_1 + a^2 g_2 + afg_3 \sin\psi + afg_4 \cos\psi + ag_5 + fg_6 \sin\psi + fg_7 \cos\psi, \\ a\dot{\psi} &= a^3 g_8 + a^2 g_9 + afg_{10} \sin\psi + afg_{11} \cos\psi + ag_{12}\Omega + ag_{13} + fg_{14} \sin\psi + fg_{15} \cos\psi \end{aligned} \tag{17}$$

where the expressions of g_i depend on the nondimensional constitutive parameters. The periodic response is obtained by searching for the fixed points of the modulation equations obtained as solutions of $\dot{a} = 0 = \dot{\psi}$. The frequency-response equation can thus be obtained in closed form as

$$\begin{aligned} \Gamma(a,\Omega) &= a^2\left((ag_3+g_6)\left(a^2g_8+ag_9+g_{12}\Omega+g_{13}\right)-\left(a^2g_1+ag_2+g_5\right)(ag_{10}+g_{14})\right)^2 \\ &+ a^2\left((ag_4+g_7)\left(a^2g_8+ag_9+g_{12}\Omega+g_{13}\right)-\left(a^2g_1+ag_2+g_5\right)(ag_{11}+g_{15})\right)^2 \\ &- f^2\left(ag_4(ag_{10}+g_{14})+g_7(ag_{10}+g_{14})-(ag_3+g_6)(ag_{11}+g_{15})\right)^2 = 0. \end{aligned} \tag{18}$$

The frequency-response function is a quadratic function of Ω, it can thus be solved to yield the solutions as

$$c_2\Omega^2 + c_1\Omega + c_0 = 0 \quad \Rightarrow \quad \Omega_{1,2} = -\frac{c_1}{2c_2} \pm \frac{\sqrt{c_1^2 - 4c_2c_0}}{2c_2}. \tag{19}$$

One can obtain the fold bifurcation points along the frequency-response curves by finding the stationary points of $\Omega(a)$ with respect to a. However, since the equation is a tenth order polynomial, its solutions are sought numerically.

2.6. Numerical Investigations

The obtained frequency-response functions allow to investigate the system response near the primary resonance. Figure 2 illustrates the frequency-response curves for different excitation levels ($f = 0.01, 0.015, 0.02$). Moreover, different kinds of hysteresis are investigated by varying the parameters of the Bouc-Wen model. In Fig. 2 the dotted-dashed lines represent the backbone curves, the dotted-dashed gray lines represent the loci of fold points and the dashed lines describe the unstable branches of the frequency-response curves. By introducing the cubic restoring term αx^3, it is possible to describe an oscillator which, for small excitation amplitudes, has a softening behavior while at

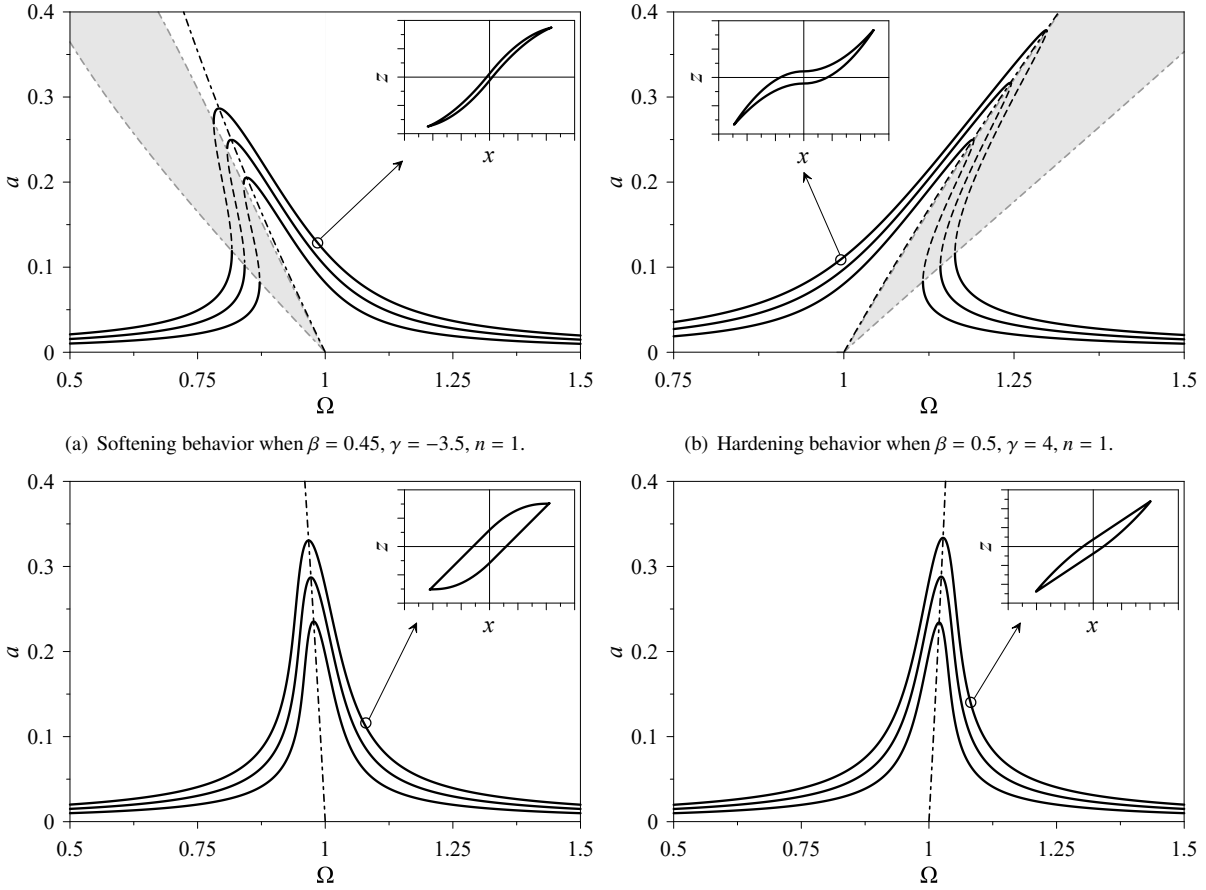

(a) Softening behavior when $\beta = 0.45$, $\gamma = -3.5$, $n = 1$.

(b) Hardening behavior when $\beta = 0.5$, $\gamma = 4$, $n = 1$.

(c) Quasi-linear behavior when $\beta = -0.45$, $\gamma = 0.45$, $n = 1$.

(d) Quasi-linear behavior when $\beta = 0.45$, $\gamma = -0.45$, $n = 1$.

Fig. 2. Frequency-response curves, backbone curves and unstable regions for three excitation levels, $f = (0.01, 0.015, 0.02)$. The adopted nondimensional material parameters are $\delta = 0.05$, $n = 1$, $\alpha = 0$.

higher amplitudes it can exhibit a hardening behavior. The results are shown in Fig. 3, where the frequency-response curves are pictured together with their corresponding backbone curves and bifurcation points. The thin black lines in Fig. 3 represent the 'exact' solution which is obtained via a path-following algorithm. The comparison between the two solutions shows a good agreement and also indicates that the dynamic response is well represented by the multiple scales solution at relatively large amplitudes. In the next section, the asymptotic procedure is extended to a two-dof system to investigate the vibration control problem.

3. Two-degree-of-freedom system

The hysteretic oscillator is coupled to a nonlinear primary structure, representing the critical mode of the structure to be controlled. The reduced-order model comprises two nonlinear oscillators. The primary system is characterized by linear damping and stiffness terms, but also by a nonlinear cubic restoring force. Its displacement is denoted by x_1. The dynamics of the hysteretic oscillator are governed by the same equations described in the previous sections. The

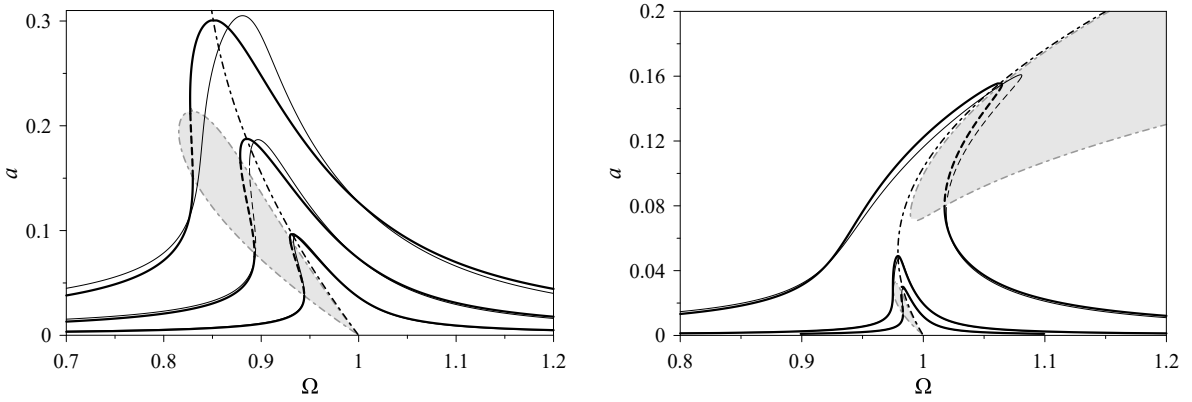

(a) $\alpha = 2$. (b) $\alpha = 20$.

Fig. 3. Frequency-response curves, backbone curves and unstable regions (grey areas) when $\xi = 0.0005$, $\delta = 0.05$, $\beta = 0.45$, $\gamma = 4$, $n = 1$. Three levels of excitation are considered, $f = (0.0002, 0.0005, 0.0075)$. Parts (a) and (b) correspond to $\alpha = 2$ and $\alpha = 20$, respectively. The thicker solid lines indicate the asymptotic solution while the thin solid lines represent the 'exact' path following solution.

nondimensional equations of motion of the two-dof system are

$$\begin{aligned} &\ddot{x}_1 + 2\,\xi_1\,\dot{x}_1 + x_1 + \alpha_1\,x_1^3 + \mu\,(\ddot{x}_1 + \ddot{x}_2) = f\cos\Omega t, \\ &\mu\,(\ddot{x}_1 + \ddot{x}_2) + \delta\,\mu\,\alpha^2\,x_2 + \mu\,\alpha^2\,\alpha_2\,x_2^3 + \mu\,\alpha^2\,(1-\delta)\,z = 0, \\ &\dot{z} = \left[1 - (\gamma + \beta\,\mathrm{sign}[z\,\dot{x}_2]|z|^n\right]\,\dot{x}_2 \end{aligned} \tag{20}$$

where ξ_1, α_1, f and Ω represent the damping ratio, the coefficient of the nondimensional cubic force and the nondimensional excitation amplitude and frequency, respectively. Besides the constitutive parameters of the Bouc-Wen model, the two-dof system depends also on μ and α representing the mass and frequency ratios between the absorber and the primary structure.

It is convenient to express the equations of motion in modal coordinates and to adopt the first-order (in time) formulation. The modal coordinates are defined as $\mathbf{x} = \Phi\,\mathbf{q}$ where the columns of $\Phi = \{\phi_{i,j}\}$ represent the modal eigenvectors related to the eigenvalue problem, and $\mathbf{p} = \dot{\mathbf{q}}$ is the vector listing the velocities. In matrix form the equations of motion become

$$\begin{aligned} &\dot{\mathbf{q}} - \mathbf{p} = \mathbf{0}, \\ &\dot{\mathbf{p}} + \mathbf{\Lambda}\,\mathbf{q} = -\mathbf{D}\,\mathbf{p} - \mathbf{f}_{\mathrm{nl}} - \mathbf{f}_z - \mathbf{f} \end{aligned} \tag{21}$$

where $\mathbf{\Lambda}$ is a diagonal matrix that collects the squared frequencies obtained from the eigenvalue problem, $\mathbf{D}$, $\mathbf{f}_{\mathrm{nl}}$ and $\mathbf{f}$ are the modal damping matrix, the modal cubic restoring force vector and the modal external load vector, respectively. $\mathbf{f}_z$ is the vector of the modal hysteresis force representing only the nonlinear part of z, since its linear contribution is absorbed in the linear problem.

4. Multiple Scales Analysis

The method of multiple scales is again employed to study the primary resonance expressed by $\Omega = \omega_1 + \epsilon\sigma_1$ occurring between the primary structure and the external excitation, but also the 1:1 internal resonance expressed by $\omega_2 = \omega_1 + \epsilon\sigma_2$ involving the two modes. The hysteresis force is treated separately, as described before, in order to obtain the Taylor series expansion up to third order. By introducing the ordering parameter ϵ, the displacements and velocities are expressed as

$$\mathbf{q} = \epsilon\,\mathbf{q}_1(t_0^*, t_1, t_2) + \epsilon^2\,\mathbf{q}_2(t_0^*, t_1, t_2) + \epsilon^3\,\mathbf{q}_3(t_0^*, t_1, t_2) \quad \text{and} \quad \mathbf{p} = \epsilon\,\mathbf{p}_1(t_0^*, t_1, t_2) + \epsilon^2\,\mathbf{p}_2(t_0^*, t_1, t_2) + \epsilon^3\,\mathbf{p}_3(t_0^*, t_1, t_2). \tag{22}$$

Since it is of interest to study the nonlinear interactions arising at higher orders, it is convenient to scale the external load and the damping terms so as to have them appear at second order, i.e., $f = \epsilon^2 \bar{f}$ and $\xi_1 = \epsilon \bar{\xi}_1$. Under these assumptions, the typical hierarchy of problems can be obtained as:

$$\begin{array}{lll} \text{Order } \epsilon: & \partial_0 \mathbf{q}_1 - \mathbf{p}_1 = \mathbf{0} & \\ & \partial_0 \mathbf{p}_1 + \Lambda\, \mathbf{q}_1 = \mathbf{0} & \end{array} \qquad \begin{array}{lll} \text{Order } \epsilon^2: & \partial_0 \mathbf{q}_2^{(i)} - \mathbf{p}_2^{(i)} = -\partial_1 \mathbf{q}_1 & \\ & \partial_0 \mathbf{p}_2^{(i)} + \Lambda\, \mathbf{q}_2^{(i)} = \mathbf{f}_2^{(i)} + \mathbf{f}_e \cos(\Omega t_0) & \end{array} \qquad \begin{array}{lll} \text{Order } \epsilon^3: & \partial_0 \mathbf{q}_3^{(i)} - \mathbf{p}_3^{(i)} = -\partial_2 \mathbf{q}_1 - \partial_1 \mathbf{q}_2^{(i)} & \\ & \partial_0 \mathbf{p}_3^{(i)} + \Lambda\, \mathbf{q}_3^{(i)} = \mathbf{f}_3^{(i)} & \end{array} \tag{23}$$

The superscript i has the same meaning of branch index as in the one-dof problem.

4.1. Linear Problem

The first order problem reduces to the linear undamped problem whose solution can be written as

$$q_{1,k} = A_k(t_1, t_2)\, \cos(\omega_k\, t_0^* + \theta_k), \quad p_{1,k} = -\omega_k\, A_k(t_1, t_2)\, \sin(\omega_k\, t_0^* + \theta_k) \quad \text{with } k = 1, 2. \tag{24}$$

To apply the procedure it is necessary to identify the time instants where the inter-branch transitions take place over the linear oscillation period. Here, the first-order displacement of the VA is governed by the two modal coordinates according to $x_{2,1} = \phi_{21}\, q_{11} + \phi_{22}\, q_{21}$. This implies that the characteristic time instants T_0 and T_1 depend on the relative phase $\Gamma_2 := \theta_2 - \theta_1 + \sigma_2\, t_1$ between the two modes. To obtain the expressions of T_0 and T_1 it is necessary to introduce the time shift $t_0^* = t_0 - \theta_1/\omega_1$, so that the first order solution becomes $x_{2,1} = \phi_{21}\, A_1\, \cos(\omega_1\, t_0) + \phi_{22}\, A_2\, \cos(\omega_1\, t_0 + \Gamma_2)$. Accordingly, the time instants are expressed as

$$\frac{\partial x_{2,1}}{\partial t_0} = 0 \quad \Rightarrow \quad T_0 = \frac{k_0\, \pi}{\omega_1} - \frac{1}{\omega_1} \arctan\left[\frac{\phi_{22} A_2 \sin\Gamma_2}{\phi_{21} A_1 + \phi_{22} A_2\, \cos\Gamma_2}\right], \tag{25}$$

$$x_{2,1} = 0 \quad \Rightarrow \quad T_1 = \frac{k_1\, \pi}{\omega_1} - \frac{1}{\omega_1} \operatorname{arccot}\left[\frac{\phi_{22} A_2 \sin\Gamma_2}{\phi_{21} A_1 + \phi_{22} A_2\, \cos\Gamma_2}\right]. \tag{26}$$

The integer numbers k_0 and k_1 represent the periodicity of the solution and must be set appropriately to obtain positive and sequential time instants over the oscillation period that spans the entire hysteresis loop. The other time instants can be obtained by the same periodicity conditions adopted for the one-dof system and are collected in the vector $\boldsymbol{\tau}$.

4.2. Modulation Equations

The procedure to obtain the modulation equations of the two-dof system mimics that described for the one-dof system. The quadratic and cubic problems are solved by imposing the solvability conditions

$$\sum_{i=1}^{4} \int_{\tau_i}^{\tau_{i+1}} \mathbf{w}_{1,k}^{\top}\, \mathbf{r}_j^{(i)}\, dt_0 = 0 \quad \text{and} \quad \sum_{i=1}^{4} \int_{\tau_i}^{\tau_{i+1}} \mathbf{w}_{2,k}^{\top}\, \mathbf{r}_j^{(i)}\, dt_0 = 0, \quad \text{with } j = 2, 3 \tag{27}$$

where $\mathbf{w}_{1,k}$ and $\mathbf{w}_{2,k}$ with $k = 1, 2$ represent the solutions of the adjoint homogeneous problem.

The response of the system can be studied by reconstituting the time derivative of the amplitudes and phases, thus arriving at the modulation equations. The relative phases are introduced as $\Gamma_1 = \sigma_1 t_1 - \theta_1$ and $\Gamma_2 = \theta_2 - \theta_1 + \sigma_2 t_1$. The modulation equations are then given by $\dot{A}_k = \epsilon \partial_1 A_k + \epsilon^2 \partial_2 A_k$ and $\dot{\Gamma}_k = \epsilon \partial_1 \Gamma_k + \epsilon^2 \partial_2 \Gamma_k$. The four equations are solved numerically by employing a path-following algorithm.

5. Numerical results

By solving the modulation equations it is possible to construct the frequency-response curves both for the primary oscillator and the absorber in terms of relative displacements x_1 and x_2, respectively. Figure 4 shows the frequency-response curves obtained for a set of parameters of the absorber chosen so as to have an equal-peak response of the primary system.

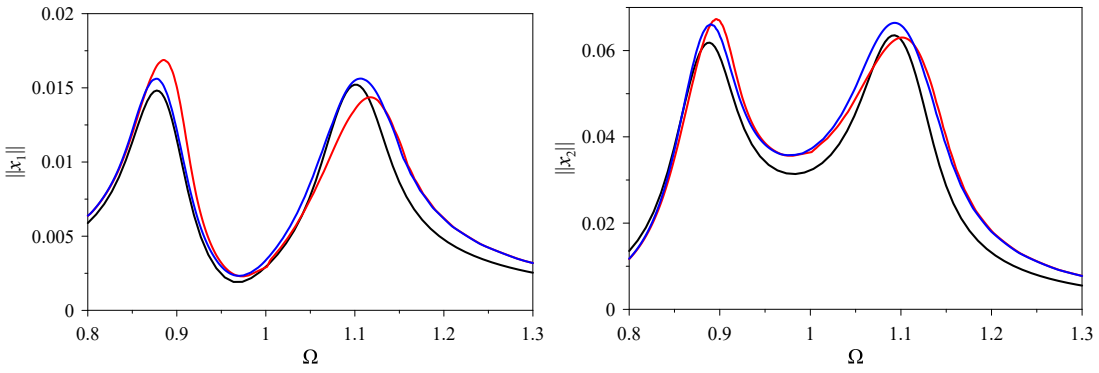

Fig. 4. Frequency-response curves both for the primary oscillator (left) and the absorber (right). The black solid line describes the numerically obtained solution. The red and blue solid lines describe the asymptotic solution truncated at second and third order, respectively.

5.1. Vibration Absorber Optimization

The obtained expressions for the displacements of the primary system and the VA allow to compute the system frequency response very efficiently. The proposed procedure is embedded within an in-house implemented differential evolutionary optimization algorithm[20], to investigate the VA design parameters that give rise to optimal vibration mitigation. This can be achieved by assuming as objective function the area below the frequency-response curves in the frequency bandwidth $[\Omega_1, \Omega_2]$, according to $\mathcal{A} = \int_{\Omega_1}^{\Omega_2} \|x_1\| \, d\Omega$ where $\|x_1\|$ denotes the amplitude of the primary system displacement. As shown in Fig. 5, a manageable optimization enabled by the analytical solution leads to a better controlled response leveraging on the hysteretic nonlinearity of the VA.

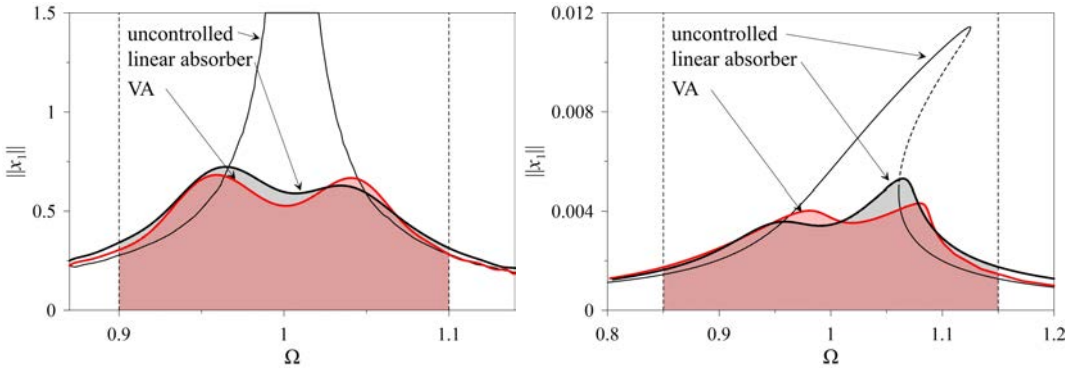

Fig. 5. Optimization of the hysteretic VA. The thin black line represents the uncontrolled structure, the thick black line is the linear VA control, the red line indicates the hysteretic VA control. Left part: the primary system is linear (i.e., linear mass-spring-damper system). Right part: the primary system is nonlinear due to a cubic restoring force.

6. Conclusions

The method of multiple scales was adopted to investigate the behavior of a nonlinear hysteretic device subject to primary resonance. The nonlinear frequency response was obtained in closed form together with the corresponding backbone curves and the loci of fold bifurcations for various hysteresis parameters. The same procedure was adopted to study the vibration control problem using a two-dof system, whereby the hysteretic VA is attached to a nonlinear primary structure. The external harmonic excitation is involved in a primary resonance with the fundamental mode, while a 1:1 internal resonance between the two modes (one associated with the primary structure and the other to the VA) takes place at the same time. The nonlinear interactions were described by constructing the frequency-response

curves both for the primary structure and the absorber, showing a good agreement with the numerically obtained solution based on path following. Finally, the asymptotic procedure was embedded into a differential evolutionary optimization scheme to derive a semi-analytic optimization strategy capable of determining the design parameters for an optimal mitigation of the dynamic response.

References

1. Frahm, H.. Device for damping vibrations of bodies. 1911.
2. Hartog, J.D.. *Mechanical Vibrations*. McGraw-Hill; 1934.
3. Brock, J.. A note on the damped vibration absorber. *Journal of Applied Mechanics* 1946;**13**:286.
4. Asami, T., Nishihara, O.. Closed-form exact solution to h_∞ optimization of dynamic vibration absorbers (application to different transfer functions and damping systems). *Journal of Vibration and Acoustics* 2003;**125**:398–405.
5. Haxton, R., Barr, A.. The autoparametric vibration absorber. *Journal of Engineering for Industry* 1972;**94**:119–125.
6. Cartmell, M., Lawson, J.. Performance enhancement of an autoparametric vibration absorber by means of computer control. *Journal of Sound and Vibration* 1994;**177(2)**:173–195.
7. Vyas, A., Bajaj, A.. Dynamic of autoparametric vibration absorbers using multiple pendulums. *Journal of Sound and Vibration* 2001; **246**:115–135.
8. Vakakis, A., Gendelman, O.. Energy pumping in nonlinear mechanical oscillators: Part iiresonance capture. *Journal of Applied Mechanics* 2000;**68**:42–48.
9. Gourc, E., Seguy, S., Michon, G., Berlioz, A.. Chatter control in turning process with a nonlinear energy sink. *Advanced Materials Research* 2013;**698**:89–98.
10. Viguié, R., Kerschen, G.. Nonlinear vibration absorber coupled to a nonlinear primary system: A tuning methodology. *Journal of Sound and Vibration* 2009;**326**:780–793.
11. Habib, G., Detroux, T., Kerschen, G.. Generalization of den hartog's equal-peak method for nonlinear primary systems. In: *Conference on Structural Nonlinear Dynamics and Diagnosis*. 2014, .
12. Habib, G., Detroux, T., Viguié, R., Kerschen, G.. Nonlinear generalization of den hartog's equal-peak method. *Mechanical Systems and Signal Processing* 2015;**52**:17–28.
13. Carpineto, N., Lacarbonara, W., Vestroni, F.. Hysteretic tuned mass dampers for structural vibration mitigation. *Journal of Sound and Vibration* 2013;**333**:1302–1318.
14. Carboni, B., Lacarbonara, W.. Nonlinear dynamic response of a new hysteretic rheological device: experiments and computations. *Nonlinear Dynamics* 2015;(DOI 10.1007/s11071-015-2305-9).
15. Carboni, B., Lacarbonara, W.. A nonlinear vibration absorber with pinched hysteresis: theory and experiments. *Journal of Engineering Mechanics* 2015;(tentatively accepted).
16. Rega, G., Lacarbonara, W., Nayfeh, A., Chin, C.. Multiple resonance in suspended cables: direct versus reduced-order models. *International Journal of Non-Linear Mechanics* 1999;**34**:901–924.
17. Lacarbonara, W., Rega, G., Nayfeh, A.. Resonant non-linear normal modes. part i: analytical treatment for structural one-dimensional systems. *International Journal of Non-Linear Mechanics* 2003;**38**:851–872.
18. Nayfeh, A., Mook, D.. *Nonlinear Oscillations*. John Wiley & Sons; 1995.
19. Lacarbonara, W., Camillacci, R.. Nonlinear normal modes of structural systems via asymptotic approach. *International Journal of Solids and Structures* 2004;**41**:5565–5594.
20. Storn, R., Price, K.. Differential evolution a simple and efficient heuristic for global optimization over continuous spaces. *Journal of Global Optimization* 1997;**11**:341–359.